Molecular Microbiology (2004) **51**(2), 407–417 doi:10.1046/j.1365-2958.2003.03861.x

Bacillus anthracis requires siderophore biosynthesis for growth in macrophages and mouse virulence

Stephen Cendrowski,[1] William MacArthur[2] and Philip Hanna[1]*

[1]*Department of Microbiology and Immunology, University of Michigan Medical School, Ann Arbor, Michigan, USA.*
[2]*GeneWorks, Inc., Ann Arbor, Michigan, USA.*

Summary

Systemic anthrax infections can be characterized as proceeding in stages, beginning with an early intracellular establishment stage within phagocytes that is followed by extracelluar stages involving massive bacteraemia, sepsis and death. Because most bacteria require iron, and the host limits iron availability through homeostatic mechanisms, we hypothesized that *B. anthracis* requires a high-affinity mechanism of iron acquisition during its growth stages. Two putative types of siderophore synthesis operons, named B*acillus* a*nthracis* *c*atechol, *bac* (anthrabactin), and *a*nthrax *s*iderophore *b*iosynthesis, *asb* (anthrachelin), were identified. Directed gene deletions in both anthrabactin and anthrachelin pathways were generated in a *B. anthracis* (Sterne) 34F2 background resulting in mutations in *asbA* and *bacCEBF*. A decrease in siderophore production was observed during iron-depleted growth in both the Δ*asbA* and Δ*bacCEBF* strains, but only the Δ*asbA* strain was attenuated for growth under these conditions. In addition, the Δ*asbA* strain was severely attenuated both for growth in macrophages (MΦ) and for virulence in mice. In contrast, the Δ*bacCEBF* strain did not differ phenotypically from the parental strain. These findings support a requirement for anthrachelin but not anthrabactin in iron assimilation during the intracellular stage of anthrax.

Introduction

Bacillus anthracis, a Gram-positive spore-forming bacillus, is the causative agent of anthrax. The spore portal of entry (cutaneous, gastrointestinal or pulmonary) determines the disease manifestation. The cutaneous form is usually self-limited resulting in a painless, oedematous lesion resolving to a thick black eschar (Friedlander, 2000). *Bacillus anthracis* spores inhaled into the lung alveoli or ingestion of contaminated food leads often to systemic anthrax (Dixon *et al*., 1999; Spencer, 2003*)*. The initial stages of anthrax are believed to be intracellular. For example, inhalation anthrax begins with engulfment of the endospores by alveolar phagocytes, which then migrate to the regional lymph nodes (Ross, 1957; Dixon *et al*., 1999; Guidi-Rontani, 2002*)*. There, it is believed, the phagocyte-associated spores germinate, and then the nascent bacilli replicate within the phagocyte and are released subsequently into the extracellular spaces of the lymph nodes. Following the release from the lymph node-associated phagocytes, the vegetative bacilli spread rapidly throughout the body via the circulation. The initial symptoms of systemic anthrax are nondescript, often characterized as 'flu-like', but without appropriate medical intervention, systemic anthrax is rapidly lethal, killing the host in just a few days from onset of symptoms (Jernigan *et al*., 2001*)*. *Bacillus anthracis* overwhelms the host, in part, by its rapid growth during infection, with reported end-stage blood titres as high as 10^9 per ml in animal models (Lincoln *et al*., 1967*)*.

The dramatic growth of *B. anthracis* during infection suggests an efficient mechanism for nutrient assimilation. For example, results from the *B. anthracis* genome project suggest the organism's metabolism is geared toward exploiting a protein-rich environment (Read *et al*., 2003). Iron acquisition from the host represents another mandatory process of bacterial pathogens. For its part, the host maintains severe limitations on free iron for prevention of oxidative damage to itself and limitation of iron availability to any invading organisms (Weinberg 2000; Goswami *et al*., 2002*)*. Thus, pathogens require specialized systems for iron expropriation (Braun and Killmann, 1999; Ratledge and Dover, 2000; Mazmanian *et al*., 2002*)*.

A few common mechanisms for iron acquisition are employed by pathogens (Wooldridge and Williams, 1993; Brown and Holden, 2002; Evans and Oakhill, 2002*)*. One method is production of high-affinity small molecule iron chelators, termed siderophores. Bacterial siderophores are produced during iron-depleted growth via non-ribosomal peptide synthetic pathways (Crosa and Walsh, 2002*)*. The siderophores are secreted and bind the insoluble ferric iron from host complexes, and then the retrieval

Accepted 3 October, 2003. *For correspondence. E-mail pchanna@umich.edu; Tel. (+1) 734 615 3706; Fax (+1) 734 764 3562.

of the Fe-siderophores is achieved by specific bacterial membrane receptor/transport complexes (Faraldo-Gomez and Sansom, 2003). Siderophore competition for host iron is exemplified by studies involving the catechol-type siderophore, enterobactin, which is at least 10-fold more efficient at chelating iron than transferrin under physiologic conditions (Harris *et al*., 1979a, b; Griffiths and Williams, 1999). The Fe–chelate association constant range for siderophores (K_a 10^{22}–10^{50}) underscores the efficiency of bacterial iron acquisition capabilities (Ratledge and Dover, 2000). A number of studies have demonstrated the importance of siderophores during infection. *Mycobacterium tuberculosis* requires the siderophore synthesis gene *mbtB* (mycobactin T) for optimal growth within MΦ-like cells (De Voss *et al*., 2000). *Klebsiella pneumoniae* and *Yersinia pestis* require their cognate siderophore operons (for aerobactin and yersiniabactin, respectively) for enhanced or complete virulence (Nassif and Sansonetti, 1986; Bearden *et al*., 1997). The *B. anthracis* genome project has annotated ORF clusters homologous to known siderophore biosynthesis, iron uptake, iron storage and metallo-regulatory genes (Read *et al*., 2003) (Table 1, Fig. 1). In the current study, genetic approaches were used to examine the role of two predicted siderophore synthesis operons in the *B. anthracis* virulence in mice as well as for growth in both iron-depleted culture medium and MΦ cultures.

Results

B. anthracis *contains two potential siderophore synthesis gene clusters*

A determination of high-affinity mechanisms for iron acquisition genes was made from the *B. anthracis* Ames strain sequence. This was accomplished in conjunction

Table 1. *B. anthracis* predicted ORFs involved in iron acquisition and regulation.

ORF Loci (BA#)	Homologues	ORF Length (bp)	Similarity (%)
Siderophore synthesis			
asb gene cluster			
1981–86	Aerobactin biosynthesis (IucA, *Escherichia coli*)	1806	45
	Aerobactin biosynthesis (IucC, *E. coli*)	1836	44
	Co-A ligase (*Bacillus halodurans*)	1236	50
	Acyl carrier protein (*Streptococcus pyogenes*)	273	65
	glycosyltransferase (*Sus scrofa*)	981	72
	hypothetical protein (*Agrobacterium tumefaciens*)	840	51
bac gene cluster	*dhb* operon of *Bacillus subtilis*		
2368–2372	2,3-dihydro-2,3-dhb dehydrogenase (DhbA)	774	75
	Isochorismate synthase (DhbC)	1197	75
	2,3-dhb-AMP ligase (DhbE)	1614	86
	Isochorismatase (DhbB)	885	79
	Serine activating enzyme (DhbF)	7155	80
Membrane-associated iron transport			
0349–0351	Ferrichrome permease (*Clostridium acetobutylicum*)	1005	88
	Permease (*Cl. acetobutylicum*)	1014	82
	Ferrichrome binding protein (*B. halodurans*)	915	80
0616–0618	Iron (III) dicitrate permease (*B. subtilis*)	1002	75
		1056	78
		819	87
4595–4597	Ferrichrome transporter (*B. subtilis*)	816	71
	Ferrichrome ABC transporter (*B. subtilis*)	1026	78
	Ferrichrome binding protein (*B. halodurans*)	945	71
4766–4767	Iron-compound binding protein (*B. halodurans*)	972	67
	Iron (III) dicitrate permease (*B. halodurans*)	2034	71
4784–4786	Ferrichrome ABC transporter (*B. halodurans*)	768	80
	Ferrichrome permease (*B. halodurans*)	981	86
	Ferrichrome binding protein (*B. halodurans*)	873	64
5327–5330	Iron ABC transporter (Yersinia pestis)	750	72
	Iron transport permease (*Y. pestis*)	1062	68
	Iron transport permease (*Y. pestis*)	1002	74
	Iron (III) binding protein (Neisseria meningitidis)	999	54
Metallo-regulatory proteins/iron storage			
0537	PerR (*B. subtilis*)	432	86
4313	Fur (*B. subtilis*)	453	92
4503	Zur (*B. subtilis*)	411	81
5296	ferritin (*B. halodurans*)	504	85

The locus numbers assigned by TIGR are listed in contiguous ranges with each consecutive locus homologue listed from top to bottom for that range. The homologue description, predicted gene length and total similarity for each ORF were derived from compiled data on the TIGR website (courtesy of Tim Read).

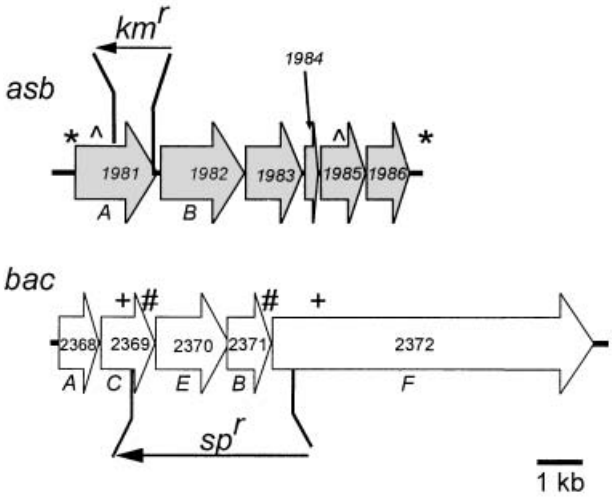

Fig. 1. *Bacillus anthracis* encodes for two distinct siderophore synthesis pathways. The putative *asb* and *bac* operons are depicted here with the TIGR assigned BA locus numbers. The gene letter designation appears below its respective ORF arrow. The relative insertion sites and orientation of the antibiotic cassettes (kanamycin, *km*^{r} spectinomycin, *sp*^{r}) are depicted (not to scale). For the *asb* gene cluster, the (*) represents primer locations used to clone the *asb* region used in the complementation plasmid (pSC109). The (∧) represents primer locations used to clone the region used in deletion of *asbA*. For the *bac* region, the (+ #) and (# +) indicate primer pairs used in cloning fragments used in a SOE technique. The (+) primers were used in the final SOE reaction.

with the *B. anthracis* genome project at the Institute for Genomic Research (TIGR). Directed searches were performed on the Ames strain genome sequence using the BLAST program TBLASTN (Altschul *et al*., 1997) resulting in the identification of several iron acquisition-related ORFs (Table 1; http://www.tigr.org). Best hits analyses using the default parameters from the NCBI/NLM BLAST website (http://www.ncbi.nlm.nih.gov/BLAST) for the Ames strain (data not shown) along with independent sequencing of homologous regions cloned from Sterne 34F2 (Fig. 1) indicated two distinct ORF clusters with similarity to siderophore synthesis enzymes. A region orthologous to the *Bacillus subtilis dhb* operon (for bacillibactin) (Rowland *et al*., 1996) was named *bac* (b*acillus* a*nthracis* c*atechol*, anthrabactin, BA2368-2372). In addition, clustered orthologues of the *E. coli* hydroxamate aerobactin *iuc* operon (Martinez *et al*., 1994) were named *asbAB (*anthrax siderophore biosynthesis, anthrachelin, BA1981-1982). The 5-gene *bac* cluster is 79% similar to the *dhbACEBF* operon of *B. subtilis* (Table 1). The strong similarity and synteny with *dhb* as well as an identical Fur box (upstream of *bacA*, not shown) suggests that *bac* encodes for iron-regulated catechol siderophore synthesis proteins responsible for a catechol siderophore similar to bacillibactin (Chao *et al*., 1966a; Bsat and Helmann, 1999; May *et al.,* 2001). The second siderophore synthesis gene cluster, *asbAB*, shares 45% similarity with genes *iucA* and *iucC*, required for the production of the hydroxamate siderophore, aerobactin in *E. coli* (de Lorenzo and Neilands, 1986). These *asbAB* ORFs are found in the Sterne and Ames strains, and at least two other wild-type *B. anthracis* strains (NWA and KrugerB), but are not found in the closely related *Bacillus cereus (10987)* (J. Ravel, pers. com.) or in *Bacillus subtilis*. In addition, the *asbAB* and the downstream ORFs (Table 1) appear clustered in operon fashion. The role of the downstream ORFs (BA1983-1986) in siderophore production is unclear; however, the location of a putative Fur box upstream of *asbA* (not shown), a potentially encoded iron regulatory protein (Fur homolog, Table 1) and the predicted domain homologies of these ORFs (Table 1) suggest a possible role in siderophore production in response to iron deprivation (Suo *et al*., 2001; May *et al.,* 2002; Rodriguez *et al*., 2002; Grifantini *et al*., 2003; Hantke *et al*., 2003). Given that *B. anthracis* encodes a plethora of high-affinity iron transport mechanism-like loci (Table 1), a focused approach on the role of the potential mediators of this uptake process, i.e. the high-affinity iron chelators produced by *B. anthracis,* was taken.

asbA *but not* bacCEBF *is required for full virulence in mice*

In order to study the roles of the siderophore ORFs, specific deletions of the *asbA* or the *bacCEBF* clusters were made in the Sterne 34F2 strain (Table 2, Fig. 1) resulting in the strains Δ*asbA* and Δ*bacCEBF* respectively. The ORF disruption made in *asbA* likely disrupts the downstream ORFs expression thought to be part of the *asb* operon as well, though no discernible ORF is detectable downstream of BA1986 for *c. 2*500 nucleotides. The spore germination and lethal toxin production characteristics as assayed by methods previously described (Dai and Koehler, 1997; Ireland and Hanna, 2002) were similar to the isogenic Sterne 34F2 strain (data not shown). A murine model of anthrax infection was employed to determine if there was a role for these siderophore operons in *B. anthracis* pathogenesis. The parental Sterne 34F2 strain, though considered attenuated for many host species, is still fully capable of producing a lethal infection in DBA/2 J and other inbred mouse strains with similar pathology seen associated with systemic anthrax (Welkos *et al*., 1986). Results for the mice infected with the parental Sterne 34F2 (Fig. 2) were in very close agreement with previous studies (Welkos *et al*., 1986). In contrast, the Δ*asbA* strain was *c.* three logs less virulent than the parental strain indicating that at least *asbA* was required for full virulence in DBA/2 J mice (Fig. 2). Similar effects on *B. anthracis* (Sterne) virulence in mice have been reported associated with the loss of lethal toxin component production (Pezard *et al*., 1991). However, the dose-dependent killing of the Δ*bacCEBF* strain (Fig. 2) was

Table 2. Bacterial strains and plasmids used in this study.

Strains	Relevant genotype	Reference/origin
Bacillus anthracis		
Sterne, 34F$_2$	pXO1$^+$, pXO2$^-$	Sterne (1937)
SC093	34F$_2$, Δ*bacCEBF::sp*^{r}	this work
SC107	34F$_2$, Δ*asbA::km*^{r}	this work
Escherichia coli		
XL1-Blue MRF′	*Δ(mcrA)183 Δ(mcrCB-hsdSMR- mrr)173 endA1 supE44 thi-1recA1 gyrA96 relA1 lac[F′proAB lacIqZΔM15 Tn10(Tet^r)]*	Stratagene
Sure	*e14– (McrA–) D(mcrCB- hsdSMR-mrr)171 endA1 supE44 thi-1 gyrA96 relA1 lac recB recJ sbcC umuC::Tn5 (Kan^r) uvrC [F′ proAB lacIqZΔM15 Tn10(Tet^r)]*	Stratagene
One Shot TOP10	*F- mcrA Δ(mrr-hsdRMS- mcrBC) 80lacZ ΔM15 ΔlacX74 deoR recA1 araD139 D (ara- leu)7697 galU galK rpsL(Str^r) endA1 nupG*	Invitrogen
CGSC 5127	GM48 (*dam-3, dcm-6*)	Marinus (1973)
CGSC 6478	GM272 (*dam-3, dcm-6*)	Palmer and Marinus (1994)
Plasmids		
pUC19	pBR322 derivative *lacZα ap*^{r}	Yanisch-Perron *et al*., (1985)
pCR-XL-TOPO	P$_{lac}$ lacZα ccdB km^r pUC$_{ori}$	Invitrogen
pKSV7	pUC$_{ori}$ pE194$_{ori(ts)}$ ap^r cm^r	Smith and Youngman, (1992)
pHP13	*pUC9$_{ori}$, pTA1060$_{ori}$ cm^r em^r*	Haima *et al*., (1987)
pDG783	pSB118::*km*^{r}	Guerout-Fleury *et al*., (1995)
pDG1726	pSB119::*sp*^{r}	Guerout-Fleury *et al*., (1995)
pSC099	pKSV7(*ΔbacCEBF::sp*^{r})	this work
pSC106	pKSV7*(ΔasbA::km*^{r}*)*	this work
pSC109	pHP13::*asb*	this work

similar to that of the parental strain indicating that these genes did not play a significant role in *B. anthracis* mouse virulence. Collectively, these results indicate that the *asb* genes encoding for a potential siderophore synthesis pathway are at least as important for *B. anthracis* growth and/or virulence during mouse infections as toxin production, but the *bacCEBF* genes, though appearing to encode for iron acquisition functions, are dispensable for *B. anthracis* survival in the DBA/2 J mouse model of infection.

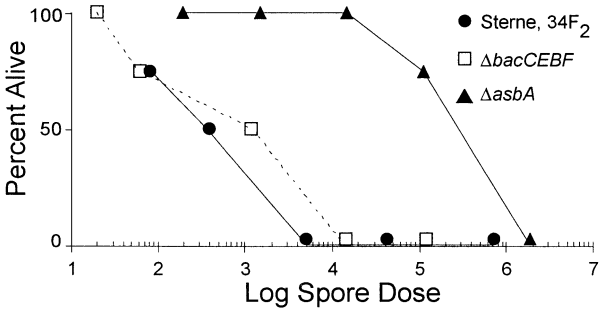

Fig. 2. The lethality of the *B. anthracis* siderophore mutant Δ*asbA* is decreased for mice. Each mouse was injected subcutaneously with a 0.1 ml suspension of spores separately for each *B. anthracis* strain. The Δ*asbA* spore dose required for total lethality was *c.* three logs higher than that needed for the Sterne, 34F2 strain. The percentage alive was calculated by dividing the dead mice by the total number of mice per dose group ($n = 4$).
The LD_{50}, calculated using the Reed and Muench method (Reed and Muench, 1938), for Sterne, 1.8×10^2; Δ*bacCEBF*, 1.3×10^2; Δ*asbA*, 2.3×10^5. All mice died within 4 days of inoculation except the Δ*asbA* 10^5 spore dose mouse that died after 7 days. For each strain, mice that succumbed to infection were cultured and the correct *B. anthracis* strains were re-isolated from spleen and/or blood samples (necropsy reports available upon request).

Both asbA *and* bacCEBF *contribute to siderophore production* in vitro*, but only* asbA *is required for growth of* B. anthracis *in iron-depleted medium*

Whereas a significant effect on *B. anthracis* virulence in mice is seen with the loss of *asbA,* but not *bacCEBF* coding regions, studies were performed to see whether these genes contributed to iron aqusition *in vitro*. For examination of iron-regulated events, a batch chelation method was employed to reduce the available iron in the described iron-depleted medium (IDM) (Cox, 1994). Four siderophore assays were utilized in attempts to elucidate the class and functionality of *B. anthracis* siderophores. It was anticipated that *asbAB* genes, which share homology to aerobactin synthesis genes, would be involved in the production of a hydroxamate class of siderophore. However, no hydroxamate-specific activities were detected (Csaky, 1948; Atkin *et al*., 1970) during the growth of *B. anthracis* Sterne under iron-depleted conditions by these methods (data not shown). In contrast, using the Arnow assay (Arnow, 1937), low iron-responsive catechol production was observed in culture supernatants during iron-depleted growth (Fig. 3). This response has been reported previously and is likely due in part to the production of a bacillibactin-like siderophore, though other non-iron related catechol molecules secreted by *B. anthracis* also

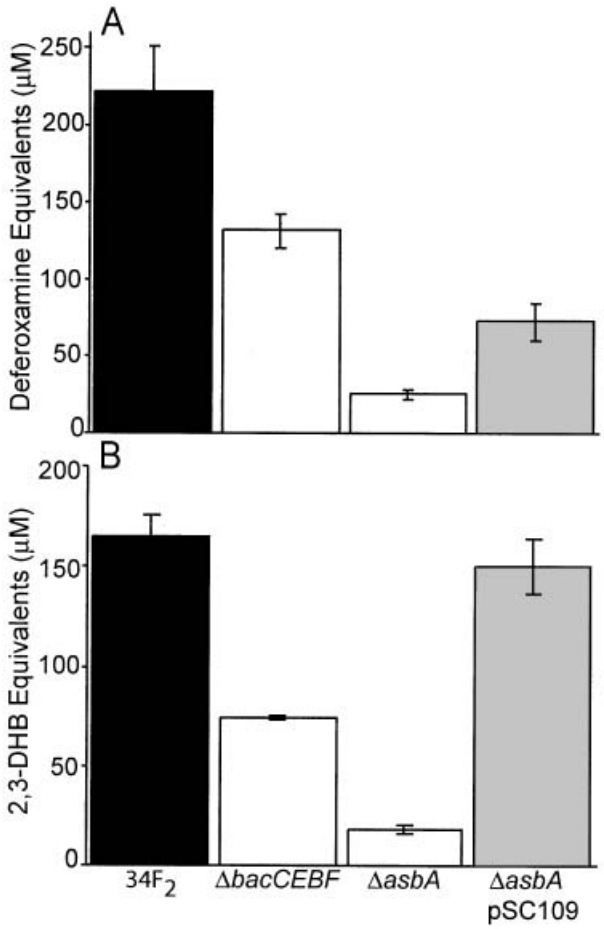

Fig. 3. *Bacillus anthracis asbA* and *bacCEBF* mutations reduce both siderophore activity and catechol detection. Culture supernatants from overnight (24 h) IDM were collected for each strain from three independent cultures. Equivalents for the CAS (A) and Arnow (B) assays were derived from a standard curve of the respective deferoxamine siderophore and 2,3-dihydroxybenzoate (DHB) catechol molecules. Measurements represented here are a mean of three separate culture supernatants grown from independent spore preps (error bars represent ± SE).

have been described (Chao *et al.*, 1966a,b; Chao *et al.*, 1967). The Arnow and the Csaky or ferric perchlorate assays are designed to detect the chemical structures characteristic for catechols and hydroxamates respectively. However, these assays might not cross-react with all non-catechol or non-hydroxamate type siderophore molecules. When the chrome azurol-S liquid (CAS) assay (Schwyn and Neilands, 1987), designed to test for general siderophore activity, was utilized, the Δ*asbA* mutant was reduced in siderophore activity by 89%. Its generation time in iron-depleted broth was 2.5-fold higher than that of Sterne 34F2 (Figs 3 and 4). The *asbA*-complemented strain's siderophore activity was increased *c.* threefold over that of the Δ*asbA* strain (Fig. 3). Likewise, the *asbA* complemented strain generation time in IDM was decreased twofold to that of the Δ*asbA* strain (Fig. 4). Despite the Δ*bacCEBF* mutant losing *c.* 41% of the parental siderophore activity, its growth in iron-depleted broth was unaffected (Figs 3 and 4). Thus, both the *asbA* and *bacCEBF* regions are required for wild-type levels of siderophore production, but only *asbA* absolutely is required during iron-depleted growth.

Growth of ΔasbA*, but not* ΔbacCEBF*, is attenuated in mouse MΦs*

Phagocytes have been shown to play a significant role during the early stages of inhalation anthrax, with spore germination and outgrowth taking place in lung-associated MΦs (Ross, 1957; Guidi-Rontani *et al.*, 1999*).* Experiments were performed to determine whether iron aquisition, via *bac* or *asb* systems, played a role in this critical establishment step. To address this, we coinfected cultured RAW 264.7 MΦs with *B. anthracis* parental or mutant strains. All strains were found to be equivalent for MΦ-spore uptake and germination (Fig. 5, and data not shown). Results with the Δ*bacCEBF* mutant indicated no defect for growth in MΦs when compared to the Sterne parental strain, with c. 10^7 viable bacteria per ml present

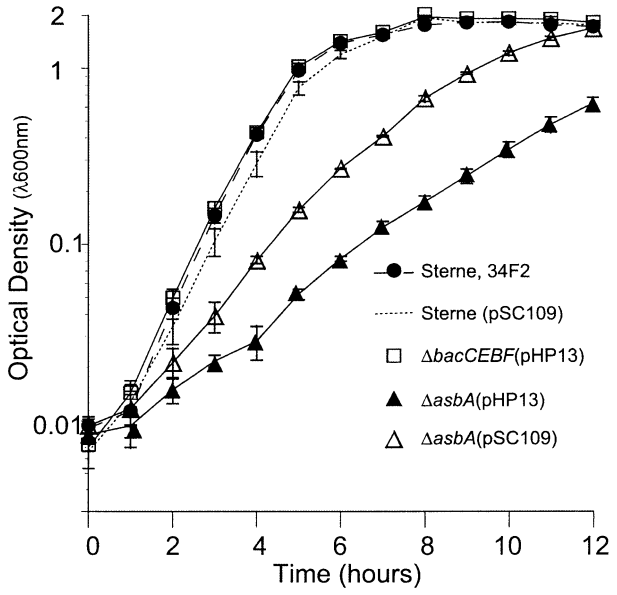

Fig. 4. Growth of the *B. anthracis* Δ*asbA* strain in iron-depleted medium is attenuated. Indicated strains were back-diluted from an IDM starter culture to a measured OD_{600} of *c.* 0.01. Time-point readings were collected at 1 h intervals. The data represented here are the mean of three separate cultures grown from independent spore preps (error bars represent ± SE).
Generation times (derived from the depicted growth curve data between 2 and 6 h) for Sterne 34F2, Δ*bacCEBF*(pHP13) and Sterne(pSC109) were all *c.* 48 min TheΔ*asbA* strain generation time was *c.* 120 min and the *asbA* complemented strain generation time was reduced to *c.* 60 min In independent *in vitro* growth studies, the generation time range in IDM plus 20 μM ferrous sulphate for Sterne, Δ*bacCEBF* and Δ*asbA* was 30–40 min (data not shown).

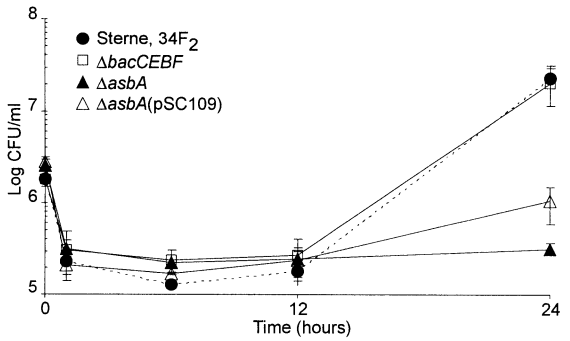

Fig. 5. MΦ-associated growth of the *B. anthracis* Δ*asbA* strain. *Bacillus anthracis* spores were added in 1 ml aliquots (*c.* 10^6 spores) onto a RAW 264.7 mouse MΦ monolayer of *c.* 10^5 (MOI 10 : 1). The total viable counts for the infection medium of each strain (0 h) were assessed. After washes and gentamicin treatment, subsequent total counts were taken at 1, 6, 12 and 24 h post infection. Time-courses depicted for each strain represent a mean of 3–5 separate infections seeded with independent spore preps (error bars represent ± SE).

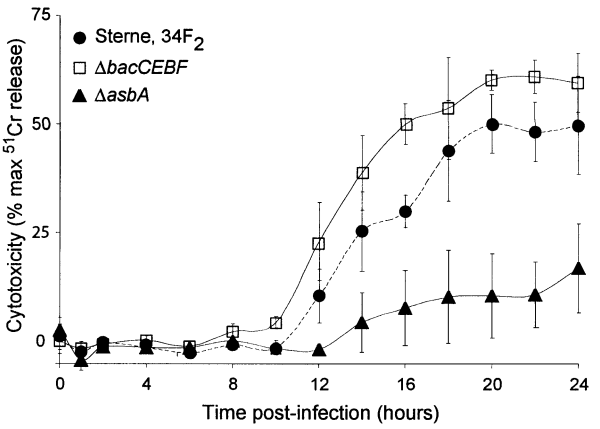

Fig. 6. The *B. anthracis* Δ*asbA* mutant is less cytotoxic to MΦ. RAW 264.7 Mϕ's were labelled with ^{51}Cr overnight in MEM + 10% HS. *B. anthracis* strain spores were then added to the labelled MΦs at an MOI of 10 : 1 as described in *Experimental procedures*. Time-points to measure MΦ ^{51}Cr release were taken every 2 h for 24 h. Data represented for each strain- MΦ infection are the mean of three separate infections seeded with independent spore preps (error bars represent ± SE).

after overnight incubation along with the observed characteristic destruction of the phagocytes (Figs 5–7; (Dixon *et al.*, 2000). In contrast, the ΔasbA mutant was severely attenuated for growth in MΦs, with no measurable increase of total bacteria (Fig. 5), and no observable MΦ cytotoxicity; though some MΦ-associated bacilli were observed after overnight infection (Fig. 7). The measurable MΦ cytotoxicity for the ΔasbA strain was also reduced c. threefold at 24 h (Fig. 6). In addition, the introduction of a plasmid encoding the asb region to the *ΔasbA* strain partially restored wild-type growth associated with this MΦ cell line (Fig. 6) and is consistent with the partial phenotypes seen previously in IDM (Figs 3 and 4) for this complemented strain. It is unclear why pSC109 only partially complements the *ΔasbA* strain phenotype, but this may be due to regulatory, indirect or other undetermined effects. The observed decreases in both *ΔasbA* MΦ-associated growth and associated cytotoxicity likely are due to the strain's overall failure to thrive in the absence of efficient siderophore-based iron acquisition, as opposed to a specific misregulation of known MΦ-lytic factors, arising from the loss of *asbA* function, e.g. anthrax lethal toxin. For instance, previous work has shown that *B. anthracis* does not require toxin production for replication associated with MΦs (Dixon *et al.*, 2000). Also, the *in vitro* induc-

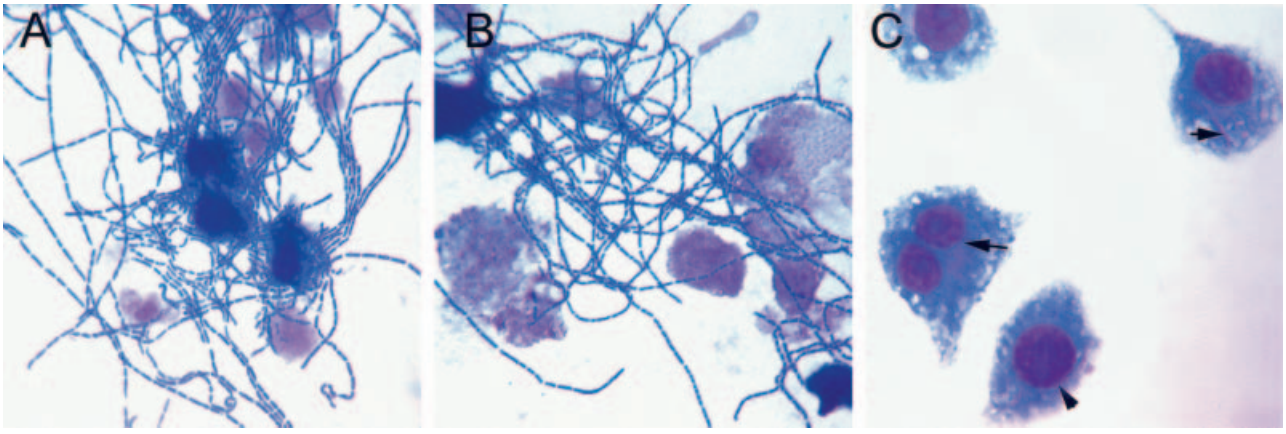

Fig. 7. Visualization of *B. anthracis*- MΦ infections by light microscopy. RAW 264.7 MΦ infections were performed as described for the viable count and cytotoxicity experiments except coverslips were included in each well. Coverslips were removed after 24 h, stained with a Wright-Giemsa like technique and photomicrographs of representative fields taken at 1000 × magnification. The Sterne 34F2 and Δ*bacCEBF* (A and B, respectively) strain infections were identical with long filamentous bacilli and the remnants of the MΦs (amorphous pink staining and pyknotic nuclei) seen. However, for the Δ*asbA* strain infections (C), few vegetative bacilli were seen and the majority of those remained associated with MΦs (arrows). The MΦ morphology in C appeared identical to that of uninfected RAW 264.7 MΦ (photo not shown).

tion of the *B. anthracis* toxin proteins, protective antigen and lethal factor (Dai *et al*., 1995*)* was unchanged from Sterne 34F2 in the *ΔasbA* mutant, after growth in IDM with CO_2, as determined by immunoblot analysis (data not shown). Collectively, these results suggest the *asbA* gene is likely a siderophore synthesis gene essential for iron-depleted growth and asb is important during the MΦ initiation step of infection. This suggests that the failure to survive the initial MΦ phase directly is related to the marked decrease in the *ΔasbA* strains virulence in mice (Fig. 2).

Discussion

The early MΦ events of anthrax have been studied primarily with respect to its well-described virulence factors, lethal toxin (LeTx) and oedema toxin (EdTx) (Mock and Mignot, 2003). Without LeTx, *B. anthracis* is rendered avirulent in many animal models (Hanna, 1998). However, LeTx-minus *B. anthracis* strains survive and replicate in association with cultured MΦs suggesting roles for additional genes during establishment of anthrax (Welkos, 1991; Dixon *et al*., 2000). The findings presented in this work implicate siderophore production as contributing to *B. anthracis* pathogenesis.

As described in *Results*, deletion of the *B. anthracis* predicted siderophore gene *asbA* attenuates virulence in mice. This may be due to an inability to grow during the early stages of infection associated with MΦs, as indicated independently with the RAW 264.7 Mϕ infections or a defect in later stages, or both. The *in vitro* evidence of the Δ*asbA* strain growth attenuation in IDM suggests that the MΦ growth defect is likely due to loss of an iron acquisition mechanism facilitated by siderophore production during infection. Despite the lack of direct evidence that *B. anthracis* obtains iron from within the MΦs, the recent findings that *M. tuberculosis* derives its iron from within MΦs and, separately, that their salicylate-derived siderophores are required during MΦ infection (De Voss *et al*., 2000; Olakanmi *et al*., 2002) support siderophore iron acquisition during intracellular growth as a credible hypothesis.

The *ΔbacCEBF* strain was decreased for overall siderophore production, but growth in IDM, MΦs and virulence in mice for this mutant was unaffected. One hypothesis, given the siderophore activity associated with the *ΔbacCEBF* mutant (Fig. 3), is that the additional siderophore anthrachelin compensates for the loss of anthrabactin production. This was supported by the attenuation of both siderophore activity and growth in IDM of the *ΔasbA* strain (Figs 3 and 4). If *asb-bac* co-expression were required for growth, then the loss of either *asb* or *bac*, should show the same phenotype. The nearly complete abrogation of total siderophore activity seen with the single disruption in the *ΔasbA* strain was unexpected (Fig. 3). Possible explanations for this include that the *asb* region may influence the expression of both anthrachelin and anthrabactin, and/or both siderophore types may contain catechol-like sidegroups that were scored by the Arnow assay. Any interplay of these regions and/or siderophore structures remains to be determined. Precedence for siderophores acting as regulatory molecules is exemplified by recent evidence from the study of *Pseudomonas aeruginosa*, which shows that the pyoverdine siderophore production is autoregulated by a cell-signalling cascade produced by pyoverdine which also regulates other virulence genes (Lamont *et al.,* 2002).

The apparent lack of effect on mouse virulence for the *ΔbacCEBF* strain was not surprising given the lack of effects seen during growth in macropahges or in low-iron medium. However, this does not necessarily preclude anthrabactin from playing a role in other host species. A finding that lends to this idea is the mutagenesis of the *Brucella abortus* catechol siderophore pathway (brucebactin) does not influence virulence in mice but induces an avirulent phenotype in cows, its primary host (Bellaire *et al*., 1999; 2003*).*

In conclusion, our studies implicate *B. anthracis* iron acquisition systems, via siderophores, as vital processes during anthrax infections. Anthrachelin (*asb*) was required for bacterial growth in low iron medium, growth in and cytotxicity to MΦs, and for mouse virulence. The catechol anthrabactin (*bac*) also was produced in response to low iron medium but was not required for growth in that medium, for growth in MΦs or for mouse virulence. The functions of other putative Fe-acquisition genes (Table 1) remain to be determined, as does exploration of anti-iron uptake systems as potential therapies for anthrax.

Experimental procedures

Plasmid and bacterial strain construction

Strains and plasmids used for this study are summarized in Table 2. The cloning and construction of plasmids were facilitated by the use of the plasmid-compatible *Escherichia coli* strains listed. Oligonucleotide primers for PCR amplification of the *asb* and *bac* regions (depicted by symbols in Fig. 1) were designed using the genomic sequence of the *B. anthracis* Ames strain (ftp://ftp.ncbi.nih.gov/GenBank/genomes/Bacteria/Bacillus_anthracis_Ames/), with the genomic template isolated from Sterne 34F2. PCR amplifications were performed using the Expand High Fidelity system (Roche) (Engineered restriction sites for all primers are underlined). The region encoding *asbA* was amplified (forward 5′-CG GGATCCGCATTATACGGTTTCCATACATCCTTTATAGAGG -3′, reverse 5′-ACCATGACAATGACATAGCGATTCTCTGGC TT-3′) (^, Fig. 1). A 2 kb *Bam*HI-*Eco*RI restriction fragment of this amplicon was cloned into pUC19. A PCR fragment of pDG783 containing the Km^r cassette (forward 5′-CCGTACG TAGATAAACCCAGCGAACCATT-3′, reverse 5′-CCGACCG

GTATCGATACAAATTCCTCGTA-3′) was then cloned into the pUC19::*asbA*. For the complementation plasmid (pSC109), a 7.5 kb fragment (*, Fig. 1) was initially cloned (forward 5′-CGGGATCCCGAGGTATACCTCTTTTGTTTAACTATTTTGG-3′, reverse 5′-AACTGCAGTACCAATCACCTCCTTATTTATA TATAAATTGTGTTAAATTTTAA-3′) using pCR-XL-TOPO per the manufacturers protocol (Invitrogen). A SOE technique as described previously (Fleming *et al*., 1995) was used to construct a pUC19::*bacCF* plasmid using the following primers (+ →#): forward 5′-CGGGATCCCATTCGAAATGACG-3′ and reverse 5′-*GGTTCTCTGCTAAATCCGC*CTAAAGAACTAGT ATT-3′ and (#→ +): forward 5′-*GCGGATTTAGCAGAGAACC* AACGG-3′, reverse 5′-CGGAATTCTTGGAGTAACAGTGAG ACGAAG-3′ (Fig. 1) (overlapping regions in italics). A PCR fragment of the Sp^r cassette (forward 5′-CCGTGTACATAAC TATAACTAATAACGTAACGTGACTGG-3′, reverse 5′-CCGTC CGGACAAGGGTTTATTGTTTTCTAAAATCTG-3′) from pDG1726 was inserted into pUC19::*bacCF*. All deletion constructs were subsequently cloned into pKSV7 (Table 2) and confirmed by sequence analysis.

All plasmids mobilized into Sterne were first passed through one of the listed methylation deficient *E. coli* strains (Table 2) (Marrero and Welkos, 1995). Plasmid preparation for, and transformation into Sterne was performed as described previously (Koehler *et al*., 1994; Weiner and Hanna, 2003) except the electroporation buffer contained 1% PEG 8000, which enhanced recovery. To facilitate the deletion of *asbA* and *bacCEBF* by homologous recombination, an allelic exchange technique was performed as follows: Sterne strains with either pSC099 or pSC106 were passed four times in 2 ml brain–heart infusion (BHI) broth aliquots with antibiotic selection at a (non-permissive) temperature range of 38°– 40°C that eliminated plasmid replication, followed by at least five passes at 30°C in BHI containing no antibiotic and 4–5 passes at the non-permissive temperature with no antibiotic. Passes were back-diluted either 10^{-2} every 12 h or 10^{-3} every 24 h, and shaken (250–300 r.p.m) in 15 ml plastic conical tubes. Final passes were prepared for sporulation as described previously (Dixon *et al*., 2000) and plated on either kanamycin or spectinomycin. Isolates were replica plated to double selection with chloramphenicol to screen for loss of the plasmid. Deletions were confirmed by Southern blot hybridizations.

Antibiotic concentrations used for selection in BHI agar/broth were: ampicillin (100 μg ml^{-1}) kanamycin (50 μg ml^{-1}) spectinomycin (100 μg ml^{-1}) chloramphenicol (5, 30 μg ml^{-1}) erythromycin (1, 100 μg ml^{-1}). The higher concentration designations shown were for for *E. coli* strains.

Infections of mice

To investigate the virulence of the siderophore knockout strains SC093 *(ΔbacCEBF::sp^r)* or SC107 *(ΔasbA::km^r)*, mice were infected with endospore preparations of these strains and compared with the parental Sterne 34F2 infection, done in parallel. The inbred mouse strain used, DBA/2 J, is susceptible to the Sterne strain (Welkos *et al*., 1986) at levels that allow for assessment of potentially avirulent Sterne mutants. Spores of the Sterne 34F2 strain and the isogenic Δ*asbA::km^r* and Δ*bacCEBF::sp^r* strains were prepared and titered as described (Dixon *et al*., 2000), then suspended in Hank's buffered salt solution (HBSS) and serial diluted 10-fold to produce spore suspensions within the range 10^2–10^7 per ml. A 0.1 ml spore dose volume was administered subcutaneously to each mouse. A total of four mice per dose-strain with a total of five serial doses per strain were used. The remaining spore dose suspensions were then plated for total viable counts (CFU ml^{-1}). All mice (including four control mice injected with sterile HBSS) were observed twice daily for 12 days at which point euthanasia was performed on all remaining mice. Upon observation of death, the carcasses were culled, and necropsies performed during which blood and/or spleen samples were taken for culture. The spore lethal dose required to kill 50% (LD50) of the mice inoculated, was estimated by the method of Reed and Muench (Reed and Muench, 1938).

Mice were housed and maintained in a humane fashion (animal welfare assurance number, A4254-01).

Infections of cultured MΦs

To assess the characteristics of the Δ*asbA::km^r* and Δ*bacCEBF::sp^r* strains under conditions mimicking the early stages of anthrax infection, a tissue culture model of MΦ-associated growth was utilized. RAW 264.7 cells, a MΦ-like transformed cell line (ATCC TIB 71) were maintained in minimal essential medium (MEM) with 10% fetal bovine serum (Gibco BRL). Upon reaching confluency in T-75 flasks (Corning), the viable RAW cells were enumerated, back diluted to ~10^5 per ml in prewarmed MEM + 10% horse serum (HS), seeded to 24-well plates at a density of ~10^5 per well and allowed to adhere overnight. The next day, the old medium was removed from the wells and spore dilutions, prepared in prewarmed MEM + 10%HS at a concentration of ~10^6 viable spores per ml were applied. Plates were centrifuged and incubated as before to optimize endospore–MΦ interaction (Dixon *et al*., 2000). At this point (30 min post infection), each well was siphoned of its medium, washed three times with prewarmed MEM (alone) then 1 ml fresh prewarmed MEM + 10%HS with 5 μg ml^{-1} of gentamicin was added to reduce the number of extracellular organisms. Gentamicin was removed after 30 min incubation, the wells were washed as before, and fresh MEM + 10% HS was applied. For assessment of total viable bacteria remaining in the co-cultures over time, the medium was removed, and a 1 ml aliquot of PBS + 0.2% saponin was added to lyse the MΦs; after vigorous pipetting and scraping this lysis buffer was removed to a sterile tube and serial diluted for total viable bacterial cell counts (CFU ml^{-1}). The timepoints taken were the initial (0), 1, 6, 12 and 24 h post infection. The infections for microscopic analysis were done identically, except sterile round microscope coverslips were added to the wells prior to MΦ seeding. The coverslips were Wright-Giemsa stained (Hema 3′, Fisher) and photomicrographs were taken at 1000 times magnification. The evaluation of cytotoxicity by measurement and calculation of percentage ^{51}Cr release was performed as before (Dixon *et al*., 2000), except infections were done as outlined above, the timepoints taken were every two hours post infection (through 24 h) and the ^{51}Cr measurements were performed on a Beckman Gamma 5500 Counting System.

B. anthracis *growth during iron limitation and its production of siderophores*

A prechelation method was used in the formulation of low-iron medium. Defined medium and salt recipes listed below were based on a previous work and applied to optimize Sterne growth under conditions of iron starvation (Puziss and Wright, 1954). A separate stock solution of defined medium and salts were made in the following concentrations: defined medium (g l^{-1}): 0.53 serine, 1.5 threonine, 1.5 valine, 3.28 leucine, 3.28 isoleucine, 1.66 aspartic acid, 4.05 glutamic acid, 2.18 arginine, 1.94 histidine, 0.22 cysteine, 0.75 methionine, 0.72 proline, 1.65 phenylalanine, 1.28 tryptophan, and 0.003 thiamine. Salts (g l^{-1}): 0.25 $MgSO_4 \cdot 7H_2O$, 0.025 $MnSO_4 \cdot H_2O$, 17.0 KH_2PO_4 and 21.8 K_2HPO_4. In addition, a 10% stock solution of casamino acids (CA), and a 20% dextrose solution were made. All were made with distilled-deionized water (MilliQ) in plastic beakers. A chelating resin (Chelex 100) was then added according to the manufacturer's batch chelation method (Bio-Rad). After the resin chelation, the stock solutions were sterile-filtered through a 0.22-μm cellulose acetate filter into a sterile plastic flask (Corning). The stock solutions were then mixed as follows with a 0.3% PIPES buffer + 0.06% NaOH solution to make the working Iron Depleted Medium (IDM): 4% of the defined medium and salts stocks, 12% of the CA and 1% of the dextrose solutions were added. This was then passed through a filter system as described before. IDM was analysed by ion-coupled plasma mass spectrometry and found to contain *c.* 100 nM total iron. To replenish iron in the IDM for comparison of growth and for overnight starter cultures, the IDM was split before filtration and a fresh ferrous sulphate solution was added to one-half at a final concentration of 20 μM. To determine the effects of iron depletion on the growth of the siderophore mutants, Δ*asbA::km*^{r} and Δ*bacCEBF::sp*^{r}, growth kinetics in IDM were assessed. To facilitate synchronized cultures between Sterne and the mutants, starter cultures *c.* 10^6 spores of each strain to 2 ml of IDM + 20 μM ferrous sulphate were incubated on a rotator (60 r.p.m.) at 37°C for 8–10 h. These cultures were centrifuged in a Sorvall 6000D swinging bucket rotor (3000 r.p.m.) for 10 min at room temperature. The spent media were siphoned off, and the pelleted cells were resuspended in sterile PBS. These cells were centrifuged again, except the pellets were resuspended in IDM then back-diluted 10^{-3} in 2 ml IDM and grown as before in 15 ml plastic conical tubes. Cultures were back-diluted in 30 ml of prewarmed IDM to a measured OD_{600} of *c.* 0.01. Time-points taken were every hour for 12 hours. All cultures contained chloramphenicol (5 μg ml^{-1}).

Complementation of the Δ*asbA* was accomplished with the pSC109 plasmid containing *asbA* along with 273 bp upstream, the putative operon region containing the clustered ORFs (Table 1, Fig. 1) and 130 bp downstream of the BA1986 ORF. The upstream region contains a characteristic RBS, possible sigma-43 and Fur box elements whereas the downstream region was predicted to contain a transcriptional terminator. No intact ORF was predicted beyond BA1986 for *c.* 2500 bp (http://www.tigr.org).

The production of siderophore activity for Sterne grown in IDM peaked after overnight incubation (data not shown), thus, 0.22 μm sterile-filtered culture supernatants from the cultures grown as described above were collected after 24 h growth and refrigerated prior to testing. The chrome azurol S (CAS) liquid assay, a general siderophore activity assay, was performed as described previously (Schwyn and Neilands, 1987). To facilitate quantification, a standard curve was established for the assay using the iron chelator deferoxamine mesylate as described previously (Courcol *et al*., 1997; data not shown). To facilitate the assessment of catechols, an indirect measure of catechol siderophore production, the Arnow assay (Payne, 1994) was utilized for the same samples above. To facilitate the quantification of catechol production by Sterne, a standard curve utilizing 2,3-dihydroxybenzoate (2,3-dhb) was established in similar fashion to the CAS-deferoxamine curve.

Acknowledgements

A debt of gratitude goes to the lab of Lynn Walter in the Geological Sciences department (University of Michigan) for iron content analysis of culture media; to Tim Read and those at TIGR making available the *B. anthracis* sequence and those at Geneworks involved in the mouse experimentation. Thanks go out to the entire Hanna group for technical help and thoughtful discussion of this work. This work was supported in part by grants from the National Institutes of Health (AI45740) and the Office of Naval Research 14001–0422, 14011–1044 and 14021–0061.

References

Altschul, S.F., Madden, T.L., Schaffer, A.A., Zhang, J., Zhang, Z., Miller, W. *et al.* (1997) Gapped BLAST and PSI-BLAST: a new generation of protein database search programs. *Nucleic Acids Res* **25:** 3389–3402.

Arnow, L.E. (1937) Colorimetric determination of the components of 3,4-dihydroxyphenylalanine-tyrosine mixtures. *J Biol Chem* **118:** 531–537.

Atkin, C.L., Neilands, J.B., and Phaff, H.J. (1970) Rhodotorulic acid from species of *Leucosporidium, Rhodosporidium, Rhodotorula, Sporidiobolus*, and *Sporobolomyces*, and a new alanine- containing ferrichrome from *Cryptococcus melibiosum*. *J Bacteriol* **103:** 722–733.

Bearden, S.W., Fetherston, J.D., and Perry, R.D. (1997) Genetic organization of the yersiniabactin biosynthetic region and construction of avirulent mutants in *Yersinia pestis*. *Infect Immun* **65:** 1659–1668.

Bellaire, B.H., Elzer, P.H., Baldwin, C.L., and Roop, R.M. 2nd (1999) The siderophore 2,3-dihydroxybenzoic acid is not required for virulence of *Brucella abortus* BALB/c mice. *Infect Immun* **67:** 2615–2618.

Bellaire, B.H., Elzer, P.H., Hagius, S., Walker, J., Baldwin, C.L., and Roop, R.M. 2nd (2003) Genetic organization and iron-responsive regulation of the *Brucella abortus* 2,3-dihydroxybenzoic acid biosynthesis operon, a cluster of genes required for wild-type virulence in pregnant cattle. *Infect Immun* **71:** 1794–1803.

Braun, V., and Killmann, H. (1999) Bacterial solutions to the iron-supply problem. *Trends Biochem Sci* **24:** 104–109.

Brown, J.S., and Holden, D.W. (2002) Iron acquisition by Gram-positive bacterial pathogens. *Microbes Infect* **4:** 1149–1156.

Bsat, N., and Helmann, J.D. (1999) Interaction of *Bacillus subtilis* Fur (ferric uptake repressor) with the *dhb* operator *in vitro* and *in vivo*. *J Bacteriol* **181:** 4299–4307.

Chao, K.-C., Hawkins, D. Jr and Williams, R.P. (1966a) Identification as protocatechuic acid of a pigment produced by *Bacillus anthracis*. *Bacteriol Proc: 20.*

Chao, K.-C., Hawkins, D. Jr and Williams, R.P. (1966b) Production of Copropophyrin III by *Bacillus anthracis*. *Bacteriol Proc: 195.*

Chao, K.-C., Hawkins, D. Jr and Williams, R.P. (1967) Pigments produced by *Bacillus anthracis*. *Fed Proc* **26:** 1532–1533.

Courcol, R.J., Trivier, D., Bissinger, M.-C., Martin, G.R., and Brown, M.R. (1997) Siderophore production by *Staphylococcus aureus* and identification of iron-regulated proteins. *Infect Immun* **65:** 1944–1948.

Cox, C.D. (1994) Deferration of laboratory media and assays for ferric and ferrous ions. *Methods Enzymol* **235:** 315–329.

Crosa, J.H., and Walsh, C.T. (2002) Genetics and assembly line enzymology of siderophore biosynthesis in bacteria. *Microbiol Mol Biol Rev* **66:** 223–249.

Csaky, T.Z. (1948) On the estimation of bound hydroxylamine in biological materials. *Acta Chem Scand* **2:** 450–454.

Dai, Z., and Koehler, T.M. (1997) Regulation of anthrax toxin activator gene (*atxA*) expression in *Bacillus anthracis*: temperature, not CO_2/bicarbonate, affects AtxA synthesis. *Infect Immun* **65:** 2576–2582.

Dai, Z., Sirard, J.C., Mock, M., and Koehler, T.M. (1995) The *atxA* gene product activates transcription of the anthrax toxin genes and is essential for virulence. *Mol Microbiol* **16:** 1171–1181.

De Voss, J.J., Rutter, K., Schroeder, B.G., Su, H., Zhu, Y., and Barry, C.E.I. (2000) The salicylate-derived mycobactin siderophores of *Mycobacterium tuberculosis* are essential for growth in macrophages. *Proc Natl Acad Sci USA* **97:** 1252–1257.

Dixon, T.C., Meselson, M., Guillemin, J., and Hanna, P.C. (1999) Anthrax. *N Engl J Med* **341:** 815–826.

Dixon, T.C., Fadl, A.A., Koehler, T.M., Swanson, J.A., and Hanna, P.C. (2000) Early *Bacillus anthracis*–macrophage interactions: intracellular survival and escape. *Cell Microbiol* **2:** 453–463.

Evans, R.W., and Oakhill, J.S. (2002) Transferrin-mediated iron acquisition by pathogenic *Neisseria*. *Biometals* **30:** 705–707.

Faraldo-Gomez, J.D., and Sansom, M.S.P. (2003) Acquisition of siderophores in Gram-negative bacteria. Nature Reviews. *Mol Cell Biol* **4:** 105–116.

Fleming, A.B., Tangney, M., Jorgensen, P.L., Diderichsen, B., and Priest, F.G. (1995) Extracellular enzyme synthesis in a sporulation-deficient strain of *Bacillus licheniformis*. *Appl Environ Microbiol* **61:** 3775–3780.

Friedlander, A.M. (2000) Anthrax: clinical features, pathogenesis, and potential biological warfare threat. *Curr Clin Top Infect Dis* **20:** 335–349.

Goswami, T., Rolfs, A., and Hediger, M.A. (2002) Iron transport: emerging roles in health and disease. *Biochem Cell Biol* **80:** 679–689.

Grifantini, R., Sebastian, S., Frigimelica, E., Draghi, M., Bartolini, E., Muzzi, A. *et al.* (2003) Identification of iron-activated and – repressed Fur-dependent genes by transcriptome analysis of *Neisseria meningitidis* group B. *Proc Natl Acad Sci USA* **100:** 9542–9547.

Griffiths, E., and Williams, R.P. (1999) *Iron And Infection: Molecular, Physiological And Clinical Aspects.* Bullen, J.J., and Griffiths, E., (eds). New York: John Wiley, pp. 99.

Guerout-Fleury, A.M., Shazand, K., Frandsen, N., and Stragier, P. (1995) Antibiotic-resistance cassettes for *Bacillus subtilis*. *Gene* **167:** 335–336.

Guidi-Rontani, C. (2002) The alveolar macrophage: the Trojan horse of *Bacillus anthracis*. *Trends Microbiol* **10:** 405–409.

Guidi-Rontani, C., Weber-Levy, M., Labruyere, E., and Mock, M. (1999) Germination of *Bacillus anthracis* spores within alveolar macrophages. *Mol Microbiol* **31:** 9–17.

Haima, P., Bron, S., and Venema, G. (1987) The effect of restriction on shotgun cloning and plasmid stability in *Bacillus subtilis* Marburg. *Mol Gen Genet* **209:** 335–342.

Hanna, P. (1998) Anthrax pathogenesis and host response. *Curr Top Microbiol Immunol* **225:** 13–35.

Hantke, K., Nicholson, G., Rabsch, W., and Winkelmann, G. (2003) Salmochelins, siderophores of *Salmonella enterica* and uropathogenic *Escherichia coli* strains, are recognized by the outer membrane receptor IroN. *Proc Natl Acad Sci USA* **100:** 3677–3682.

Harris, W.R., Carrano, C.J., Cooper, S.R., Sofen, S.R., Avdeef, A.E., McArdle, J.V. *et al.* (1979a) Coordination chemistry of microbial iron transport compounds. 19. Stability constants and electrochemical behavior of ferric enterobactin and model complexes. *J Am Chem Soc* **101:** 6097–6104.

Harris, W.R., Carrano, C.J., and Raymond, K.N. (1979b) Spectrophotometric determination of the proton-dependent stability constant of ferric enterobactin. *J Am Chem Soc* **101:** 2213–2214.

Ireland, J.A., and Hanna, P.C. (2002) Macrophage-enhanced germination of *Bacillus anthracis* endospores requires gerS. *Infect Immun* **70:** 5870–5872.

Jernigan, J.A., Stephens, D.S., Ashford, D.A., Omenaca, C., Topiel, M.S., Galbraith, M. *et al.* (2001) Bioterrorism-related inhalational anthrax: the first 10 cases reported in the United States. *Emerg Infect Dis* **7:** 933–944.

Koehler, T.M., Dai, Z., and Kaufman-Yarbray, M. (1994) Regulation of the *Bacillus anthracis* protective antigen gene: CO_2 and a trans-acting element activate transcription from one of two promoters. *J Bacteriol* **176:** 586–595.

Lamont, I.L., Beare, P.A., Ochsner, U., Vasil, A.I., and Vasil, M.L. (2002) Siderophore-mediated signaling regulates virulence factor production in *Pseudomonas aeruginosa*. *Proc Natl Acad Sci USA* **99:** 7072–7077.

Lincoln, R.E., Walker, J.S., Klein, F., Rosenwald, A.J., and Jones, W.I. Jr (1967) Value of field data for extrapolation in anthrax. *Fed Proc* **26:** 1558–1562.

de Lorenzo, V., and Neilands, J.B. (1986) Characterization of *iucA* and *iucC* genes of the aerobactin system of plasmid ColV-K30 in *Escherichia coli*. *J Bacteriol* **167:** 350–355.

Marinus, M.G. (1973) Location of DNA methylation genes on the *Escherichia coli* K-12 genetic map. *Mol Gen Genet* **127:** 47–55.

Marrero, R., and Welkos, S.L. (1995) The transformation frequency of plasmids into *Bacillus anthracis* is affected by adenine methylation. *Gene* **152:** 75–78.

Martinez, J.L., Herrero, M., and de Lorenzo, V. (1994) The organization of intercistronic regions of the aerobactin operon of pColV-K30 may account for the differential expression of the *iucABCD iutA* genes. *J Mol Biol* **238:** 288–293.

May, J.J., Wendrich, T.M., and Marahiel, M.A. (2001) The *dhb* operon of *Bacillus subtilis* encodes the biosynthetic template for the catecholic siderophore 2,3-dihydroxybenzoate-glycine-threonine trimeric ester bacillibactin. *J Biol Chem* **276:** 7209–7217.

May, J.J., Kessler, N., Marahiel, M.A., and Stubbs, M.T. (2002) Crystal structure of DhbE, an archetype for aryl acid activating domains of modular nonribosomal peptide synthetases. *Proc Natl Acad Sci USA* **99:** 12120–12125.

Mazmanian, S.K., Ton-That, H., Su, K., and Schneewind, O. (2002) An iron-regulated sortase anchors a class of surface protein during *Staphylococcus aureus* pathogenesis. *Proc Natl Acad Sci USA* **99:** 2293–2298.

Mock, M., and Mignot, T. (2003) Anthrax toxins and the host: a story of intimacy. *Cell Microbiol* **5:** 15–23.

Nassif, X., and Sansonetti, P.J. (1986) Correlation of the virulence of *Klebsiella pneumoniae* K1 and K2 with the presence of a plasmid encoding aerobactin. *Infect Immun* **54:** 603–608.

Olakanmi, O., Schlesinger, L.S., Ahmed, A., and Britigan, B.E. (2002) Intraphagosomal *Mycobacterium tuberculosis* acquires iron from both extracellular transferrin and intracellular iron pools: impact of interferon-gamma and hemochromatosis. *J Biol Chem* **277:** 49727–49734.

Palmer, B.R., and Marinus, M.G. (1994) The dam and dcm strains of *Escherichia coli* – a review. *Gene* **143:** 1–12.

Payne, S.M. (1994) Detection, isolation, and characterization of siderophores. *Methods Enzymol* **235:** 329–344.

Pezard, C., Berche, P., and Mock, M. (1991) Contribution of individual toxin components to virulence of *Bacillus anthracis*. *Infect Immun* **59:** 3472–3477.

Puziss, M., and Wright, G.G. (1954) Studies on immunity in anthrax. 4. factors influencing elaboration of the protective antigen of bacillus anthracis in chemically defined media. *J Bacteriol* **68:** 474–482.

Ratledge, C., and Dover, L.G. (2000) Iron metabolism in pathogenic bacteria. *Annu Rev Microbiol* **54:** 881–941.

Read, T.D., Peterson, S.N., Tourasse, N., Baillie, L.W., Paulsen, I.T., Nelson, K.E. *et al.* (2003) The genome sequence of *Bacillus anthracis* Ames and comparison to closely related bacteria. *Nature* **423:** 81–86.

Reed, L.J., and Muench, H. (1938) A simple method of estimating fifty per cent endpoints. *Am J Hyg* **27:** 493–497.

Rodriguez, G.M., Voskuil, M.I., Gold, B., Schoolnik, G.K., and Smith, I. (2002) *ideR*, an essential gene *Mycobacterium tuberculosis*: role of IdeR in iron-dependent gene expression, iron metabolism, and oxidative stress response. *Infect Immun* **70:** 3371–3381.

Ross, J.M. (1957) The pathogenesis of anthrax following the administration of spores by the respiratory route. *J Path Bact* **73:** 485–494.

Rowland, B.M., Grossman, T.H., Osburne, M.S., and Taber, H.W. (1996) Sequence and genetic organization of a *Bacillus subtilis* operon encoding 2,3-dihydroxybenzoate biosynthetic enzymes. *Gene* **178:** 119–123.

Schwyn, B., and Neilands, J.B. (1987) Universal chemical assay for the detection and determination of siderophores. *Anal Biochem* **160:** 47–56.

Smith, K., and Youngman, P. (1992) Use of a new integrational vector to investigate compartment-specific expression of the *Bacillus subtilis* spoIIM gene. *Biochimie* **74:** 705–711.

Spencer, R.C. (2003) Bacillus anthracis. *J Clin Pathol* **56:** 182–187.

Sterne, M. (1937) The effects of different carbon dioxide concentrations on the growth of virulent anthrax strains. *Onderstepoort J Vet Sci Anim Ind* **9:** 49–67.

Suo, Z., Tseng, C.C., and Walsh, C.T. (2001) Purification, priming, and catalytic acylation of carrier protein domains in the polyketide synthase and nonribosomal peptidyl synthetase modules of the HMWP1 subunit of yersiniabactin synthetase. *Proc Natl Acad Sci USA* **98:** 99–104.

Weinberg, E.D. (2000) Modulation of intramacrophage iron metabolism during microbial cell invasion. *Microbes Infect* **2:** 85–89.

Weiner, M.A., and Hanna, P.C. (2003) Macrophage-mediated germination of *Bacillus anthracis* endospores requires the gerH operon. *Infect Immun* **71:** 3954–3959.

Welkos, S.L. (1991) Plasmid-associated virulence factors of non-toxigenic (pX01-) *Bacillus anthracis*. *Microb Pathogenesis* **10:** 183–198.

Welkos, S.L., Keener, T.J., and Gibbs, P.H. (1986) Differences in susceptibility of inbred mice to *Bacillus anthracis*. *Infect Immun* **51:** 795–800.

Wooldridge, K.G., and Williams, P.H. (1993) Iron uptake mechanisms of pathogenic bacteria. *FEMS Microbiol Rev* **12:** 325–348.

Yanisch-Perron, C., Vieira, J., and Messing, J. (1985) Improved M13 phage cloning vectors and host strains: nucleotide sequences of the M13mp18 and pUC19 vectors. *Gene* **33:** 103–119.